Engineering and Technology Journal

Parametric Optimization of Laser Conduction Welding between Stainless Steel 316 and Polyethylene Terephthalate Using Taguchi Method

Marwa A. Khioon [a], **Kadhim A. Hubeatir**[*] [a] [iD] **, Mohanned M. AL-Khafaji** [b] [iD]

[a]Laser and Optoelectronics Engineering Dept, University of Technology-Iraq, Alsina'a Street, 10066 Baghdad, Iraq.
[b]Production and Metallurgical Engineering Dept, University of Technology-Iraq, Alsina'a Street, 10066 Baghdad, Iraq.
*Corresponding author Email: Kadhim.A.Hubeatir@uothechnology.edu.iq

HIGHLIGHTS

- The study showed the effectiveness of using Nd:YAG laser in welding dissimilar materials.
- The study results indicated that all the used parameters affected the joint force. However, the energy density had the highest effect among the other parameters, followed by the pulse duration and the welding speed.
- The bubble formation in the polymer side led to the weakening of the joint force. However, it can be avoided by distributing the laser energy equally on the weld line.

ARTICLE INFO

Handling editor: Makram A. Fakhri

Keywords:

Laser Conduction Welding; SUS316/PET Dissimilar Joining; Shear Test; Joint Force Taguchi Method.

ABSTRACT

A pulsed Nd:YAG laser with a fiber optic delivery system was used to accomplish a dissimilar joining of 316 stainless steel (SUS316) to polyethylene terephthalate (PET). Laser Conduction Welding (LCW) was applied as a welding technique to achieve a lap metal/polymer joint by applying the laser from the metal side. The heat was transferred from the metal layer to the polymer layer, which caused the melting and then solidifying of the polymer at the interface. The effect of three welding parameters, laser energy density, pulse duration, and welding speed, on joint force, was studied and discussed. To measure the joint force tensile shear test was conducted. Furthermore, the Taguchi method was used as a design experiment method to optimize the welding parameters by designing an orthogonal L9 matrix. The signal-to-noise ratio of each trial was calculated and plotted. The best welding parameters that gave the highest joint force were achieved. The maximum tensile force obtained was 525 N at 250 J/cm^2 energy density, 15 ms pulse duration, and 20 mm/min welding speed. Finally, the comparison between the weakest and the strongest joints was carried out to show the difference between welding with the optimal parameters and any other set of parameters.

1. Introduction

Recently combined dissimilar joints such as different metals, polymers, and metal to polymer joints are highly demanded since these joints combine the advantages of the two materials. Further, these joints aim to enhance production in industrial fields such as the automobile, aerospace, and construction industries [1]. Polymers exceed metal or ceramic in some applications due to anti-fatigue properties, high fracture toughness, excellent strength-to-weight ratio, and low cost. Polymers are mainly categorized into rubber, plastic, and fiber [2]. Employing plastic in manufacturing is evident due to its lightweight, low density, good impact resistance, good insulation and low thermal conductivity, easy forming capability, and low costs [2,3]. However, metals characterized by high strength and high thermal conductivity make them suitable materials for industrial production [4].

Achieving a good hybrid joint needs an efficient joining method with fewer defects. Using lasers in welding primarily started in the 1960s. Welding with lasers increased due to its distinct features over conventional welding techniques, such as no contact, high energy density, small heat-affected zone, precise and high-quality weld, and high flexibility [5,6].

Laser welding has laser conduction mode and keyhole mode. These two modes decide the interaction of laser radiation with materials in welding. Keyhole mode has deep penetration and high welding speeds, whereas conduction mode is more stable with higher quality welds and no defects or spatter. The main difference between the two welding modes is the power density applied to the welding area [6,7]. According to Al-Kazzaz et al., it is possible to change between the two modes by adjusting and

1642

tuning the welding parameters of power density and spot size [8]. Also, Assuncao et al. [7] conducted a study that indicated a transition mode between the conduction and keyhole welding mode. They reached this result by studying the effect of power density that relied on interaction times, beam diameters, and penetration depth. Furthermore, Chelladurai et al. [9] studied the transition between welding modes based on the laser pulse duration effect on the penetration depth. In laser conduction mode, the laser energy is transferred to the material through the surface due to conduction. In this case, minimal vaporization occurs, a more stable melt pool is produced, and a better surface finish is obtained [10].

In the laser welding process, there are four main dominant lasers. These lasers are Diode, Nd:YAG, Fiber, and CO_2 laser. These lasers share the same infrared spectrum [11]. Nd:YAG laser was chosen in this study owing to its several advantages. It firstly emits in the near-infrared region with the range of 1030–1070 nanometers. Consequently, the metals show better absorbance to this wavelength and less reflectance. It secondly operates in both continuous and pulsed modes [12]. It is thirdly capable of delivering laser beams through optical fibers, thus making it more desirable in robotic or multi-axis laser welding applications. Finally, it is characterized by high reliability, high efficiencies, and excellent beam quality [6].

Many studies have been performed about joining dissimilar materials using lasers. However, few of them talked about joining metals to polymers by laser conduction welding. Anawa et al. [13] used a keyhole welding laser to join different metals: AISI 316 stainless steel and AISI 1009 low carbon steel. Continuous-wave (CW) CO_2 was applied. The parametric investigation was carried out, including laser power, welding speed, and defocusing distance as input parameters. Taguchi method was used to optimize the process parameters in that study. Results indicated that the heat-affected zone and the welding pool could be controlled using the optimal parameters. In addition, the chosen laser power could affect the HAZ directly. Miyashita et al. [14] compared joining PET with 304 stainless steel (SUS304) and Polycarbonate (PC) with 304 stainless steel. Pulsed Nd:YAG laser was applied in that study. Weld-ability and shear tensile strength were also measured. SUS304/PET joint showed better results than SUS304/PC, like higher joint strength and wider weldability. The welding mode is not mentioned in this study; however, results and the existence of pores indicate that with less heat, the conduction mode is dominated until the heat increases, in which the mode is changed to keyhole mode. Hussein et al. [15] carried out a parametric investigation of the PMMA/SUS304 lap joint using a pulsed Nd:YAG laser. They used two different welding methods depending on the laser's direction: laser transmission welding and laser conduction welding. The results showed that in the case of laser conduction welding, the rise in thermal input heat increased the joint strength and the bead width. However, more increases in thermal input heat cause a decrease in strength. Liu et al. [2] succeeded in joining 316L to PET by optimizing laser power and pulse duration. They studied the influence of surface texture and ultrasonic on joint strength. A shear test was conducted to measure the joint strength. It was concluded that both processes increased the strength and improved the joint. Huang et al. [16] examined the influence of welding parameters such as laser peak power, welding speed, spot diameter, pulse duration, pulse frequency, and argon gas flow rate on joint performance of SUS304/PMMA joints using a pulsed Nd: YAG laser. According to the shear test results welding speed and pulse duration have the highest effect on the joint strength.

The previous studies presented how understanding the laser process parameters is essential to achieving the best joint. The key factor for optimizing and the success of laser joining processes are adjusting these parameters. Consequently, this study focuses on the joint force of the welding joint in laser conduction welding affected by the welding parameters. The aim is to control and optimize the process parameters to achieve the best joint force.

2. Experimental Section

2.1 Materials Preparation

In this study, as mentioned before, two dissimilar materials were joined together; the metal material was 316 stainless steel with dimensions (100 mm, 15 mm, 0.8 mm), while the polymer was PET sheets with dimensions (100 mm, 15 mm, 0.9 mm). Polyethylene terephthalate is a semicrystalline thermoplastic characterized by excellent wear and good heat resistance, electrical insulation, low coefficient of friction, low dielectric constant, and low cost [17,18].

Before welding, the sheets were cut according to the dimensions required using a Fiber laser cutting device to cut the stainless steel and a CO_2 laser cutting device to cut the PET. All specimens were cleaned with alcohol, wiped, and left to dry. SUS316 was placed as the upper layer during the welding process, while the lower layer was PET, thus forming together a lap joint as illustrated in Figure (1).
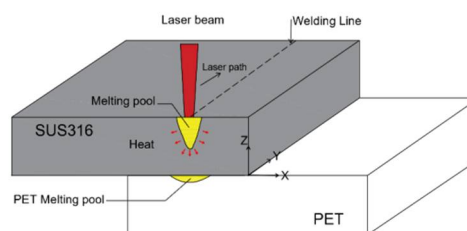
Figure 1: SUS316/PET lap joint diagram
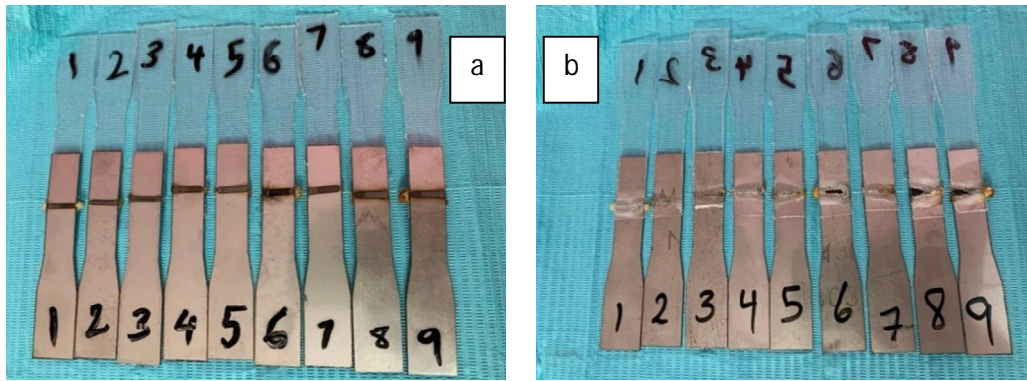
Figure 2: A lap joint of SUS316 and PET

Figure (2a) shows the specimens after welding in a lap joint from the metal side, the side where the laser is exposed. At the same time, Figure (2b) shows the welding shape from the polymer side.

2.2 Experimental Design

A pulsed Nd:YAG laser with a fiber optic delivery system was used. The maximum pulse energy density was 300 J/cm², and the wavelength was 1064 nm. The spot size of the lens was 3mm. In this experiment, the laser handpiece remained fixed, and a CNC X-Y-Z table was employed to move the specimens. The specimens were mounted on the CNC worktable, moving along the y-axis only to achieve a welding line. The standoff distance (z-axis) was fixed, which is the perpendicular distance between the laser handpiece and the surface of the metal. It was set to be 40mm; this led to a constant spot size because the beam spot area depended on the change of the standoff distance. Several parameters were also considered constant, such as the pulse reptation rate, which was 2Hz representing the maximum value the device can provide. A clamping device was developed for three significant reasons. Firstly, compress the two materials together to eliminate the air gap between them. Secondly, ensure intimate contact to allow the heat to be transferred at the interface between the two materials. Thirdly, to enhance the weld quality. The clamping force was set fixed as 2.85N. Figure (3) displays the study's experimental setup.

1. The laser handpiece
2. Zimmer cooling hose
3. CNC worktable
4. The clamping templates
5. The clamping measuring device
6. Computer interface
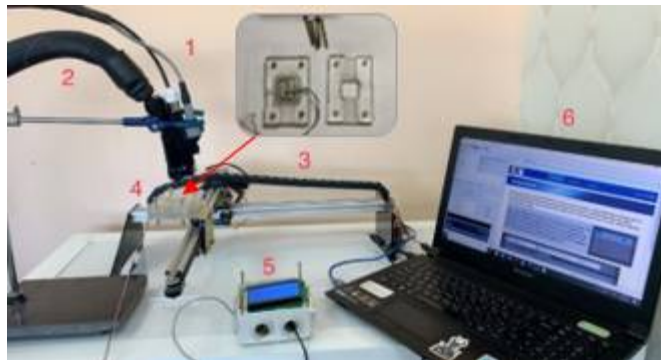
Figure 3: The experiment setup

Two microscopes were used to take images of the joints after the welding process. First, a digital microscope took the images of the weld area from the polymer side. In contrast, high-resolution images for the joint interface between SUS316 and PET were taken with a MEIJI microscope with a magnification of 50X to take a close view of the joint interface.

2.3 Selection of Parameters

To control the input heat at the weld zone, it is essential to control the laser and process parameters first, such as laser pulse energy density and laser interaction time. Laser pulse energy density is a function of laser average power and beams spot area according to the following equation [19].

$$E_a = \frac{I \cdot \tau \cdot PRR}{v \cdot \omega} = \frac{E_{pulse}}{v \cdot \omega \cdot PRT} = \frac{P_{av}}{v \cdot \omega} \; (J/cm2) \tag{1}$$

Where:
    I: Intensity (W/cm²)
τ: Pulse duration (ms)
PRR: Pulse repetition rate (Hz)
E_{pulse}: Pulse energy (J)
PRT: Pulse repetition time (s)
P_{av}: Average power (w)

υ: Scanning speed (cm/s)

ω: Laser spot size (cm)

While parameters like the welding speed, pulse duration, and pulse repetition rate can control the laser interaction time. Input parameters like pulse energy density, pulse duration, and welding speed were chosen as input variables in this study to perform the experiments. Several experiments were carried out before reaching the final values of the input parameters. These experiments aimed to determine the limits of the welding parameters. Unfortunately, achieving a weld out the range of these limits was impossible. Taguchi Method designed the selected input parameters. Classic parameters optimization methods are impractical because they are complicated to deal with. On the other hand, the Taguchi method, with its distinctive design of orthogonal arrays, proved its effectiveness in determining the optimal process parameters. It analyzed the experiment to be established with a small number of experiments. L9 orthogonal array was applied, and the parameters represented by three factors were varied into three levels, as shown in Table 1.

Table 1: Range of the variable parameters

Input parameters	Level 1	Level 2	Level 3
Energy density (J/cm²)	200	250	300
Speed (mm/min)	20	30	40
Pulse duration (ms)	5	10	15

3. Results and Discussion

3.1 Shear-Tensile Test

In this study, the welding quality of dissimilar materials was judged by shear force. The tensile test was conducted to estimate laser conduction welding joints between SUS316 and PET using a universal tensile test machine. The force is considered the maximum tensile load that the joint can withstand. Selecting and adjusting the welding parameters is essential in obtaining better joint force. Laser energy density, pulse duration, and welding speed were input parameters, whereas joint force was taken as the output variable. This study's primary aim was the optimum welding parameters that produce the best joint force. Table 2 displays all sets of input parameters and the values of the measured joint force, which represent the responses.

3.2 The Signal to Noise Analysis

Taguchi method was applied to design this experiment using an L9 orthogonal array which consisted of three columns and nine rows. This means that nine experiments were accomplished. The experiments were designed using "Minitab 19" Software. First, the signal-to-noise ratio (S/N) for each level of process parameters was determined by relying on the S/N analysis. To evaluate the effect of each factor on the joint force, the S/N ratio was calculated. Then, the S/N ratio and the means were plotted for all the input parameters, as shown in Figures (4) and (5). The rule of the S/N ratio for the joint force is considered the larger, the better. This was calculated using the equation below [20] [21]:

$$\frac{S}{N} = -10\, log_{10} \left[\frac{1}{n} \sum_{i=1}^{n} \frac{1}{y_i^2} \right] \qquad (2)$$

Where:

y: the result of the response

i: the number of experiments

n: the number of trials for each experiment

A higher S/N ratio coincided with a better response. Consequently, the highest S/N ratio was the optimal level of welding parameters. Table 2 indicates the Taguchi design of the experiment and the calculated S/N ratio.

Table 2. The input parameters, responses, and S/N ratio

Experiment No.	Energy density (J/cm²)	Pulse duration (ms)	Speed (mm/min)	Joint force (N)	S/N ratio
1	200	5	20	425	52.5678
2	200	10	30	75	37.5012
3	200	15	40	395	51.9319
4	250	5	30	390	51.82129
5	250	10	40	400	52.0412
6	250	15	20	525	54.4032
7	300	5	40	130	42.2789
8	300	10	20	85	38.5884
9	300	15	30	170	44.6089

It is obvious from Table (2) that the S/N ratio decreased sharply for both the second and the eighth joints. For the second joint, this result might be attributed to the low energy density with pulse duration and welding speed that gave the lowest S/N ratio according to the plotted S/N ratio shown in Figure (4). It would be hard to obtain a strong joint with such a parameter set. On the other hand, the set of parameters used in the eighth joint differed. The pulse duration applied in this experiment gave the highest S/N ratio, as shown in Figure (4). Nevertheless, both the energy density and the speed showed the lowest signal ratio. It

can also be seen that both joints had low force compared to the other joints. However, the sixth joint with the best joint force was obtained by applying the best parameters, thus having the highest S/N ratio.

3.3 The Effect of Process Parameters on Joint Force

Figure (4) shows the S/N ratio plot. According to the plot, the maximum response value was at the middle level of energy density. Therefore, the energy density was the main factor that affected the response, followed by pulse duration. Finally, welding speed had the lowest effect. The Main effects plot for S/N ratios suggested that the levels of variables would maximize the joint force and were robust against variability due to noises, as indicated in Figure (4). The best energy density that gave the highest S/N ratio was 250 J/cm^2, whereas the S/N ratio dropped sharply at 300 J/cm². However, choosing 300 J/cm² energy density in the set of parameters might affect the obtained results. This finding proved that the highest energy density is not always essential to gaining good results. In the pulse duration case, the long pulse duration of 15 ms showed the greatest S/N ratio, whereas the 10 ms showed the lowest S/N ratio. Finally, both the high and low welding speeds represented by 40 mm/min and 20 mm/min, respectively, gave approximate values of the S/N ratio, while 30 mm/min showed the lowest S/N value.
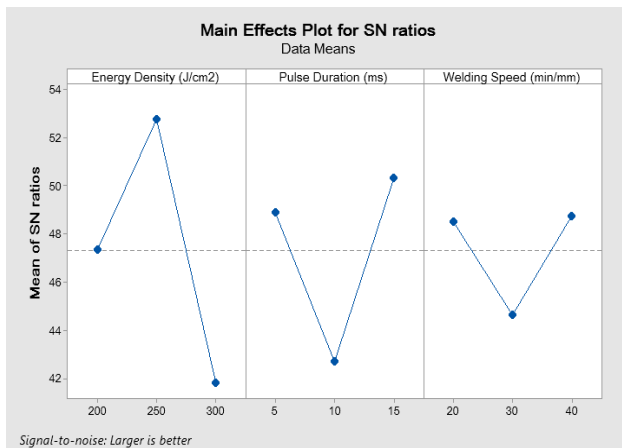
Figure 4: The S/N ratio of the joint force
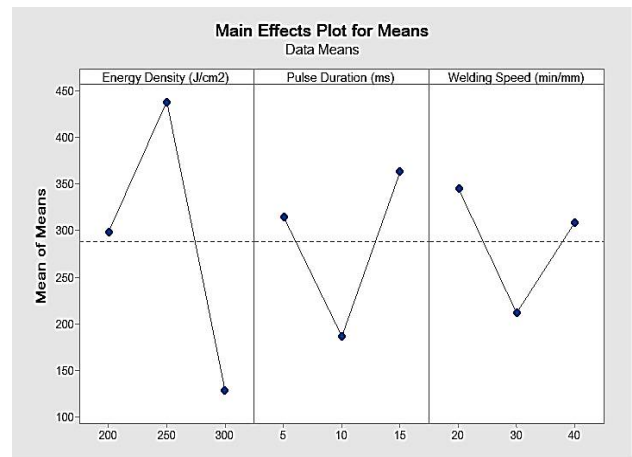
Figure 5: The mean of means plot

Figure (5) shows that the mean of the responses of 250 J/cm^2 energy densities gave the highest joint force among the other energy densityies. Also, the joint force increased firstly and then decreased with the energy density increase. Moreover, the excessive energy applied to the welding area produces the lowest force, leading to a weak joint. The joining force dropped when the pulse energy density was 300 J/cm^2. This is due to the thermal decomposition that resulted from the high energy absorbed by PET.

On the other hand, the long pulse duration of 15 ms produced tough joints compared to the short and medium pulses. The slower speeds represented with 20 mm/min produced the best joint force among the other speeds because they provided more interaction time between the laser beam and the joint area, which means more pulses in each welding line.

According to the shear test results and the S/N ratios, the optimum welding parameters were the energy density of 250 J/cm2, the welding speed of 20 mm/min, and the pulse duration of 15 ms. The largest shear stress measured was 525 N.

3.4 Comparing the Strongest and the Weakest Joint

The sixth experiment of the L9 orthogonal array had a set of parameters (250 J/cm2, 15 ms, and 20 mm/min). These parameters represented the input parameters that gave the best output result, which was the highest joint force. While in the second experiment, the lowest joint force was produced when the parameters were (200 J/cm2, 10 ms, and 30 mm/min). Figure (6) illustrates the digital microscopic morphology of the two joints given by the second and sixth experiments of the L9 orthogonal array. The most robust joint was presented in Figure (6a). The weakest one shown in Figure (6b) indicated a clear difference between the two joints representing the generation of air bubbles in the joint, which reduced the joining force. The bubbles in the molten pool were attributed to the thermal degradation of the melted polymer in the joining process, according to Jiao et al. [22] and Noh et al. [23]. Also, the bubbles were formed in the melted PET near the interface and adhered to the SUS316 surface. Therefore, they could not escape into the air from the molten layer. In addition, the formation of the bubble could be controlled by distributing the laser heat equally by adjusting the incident laser energy on the material.
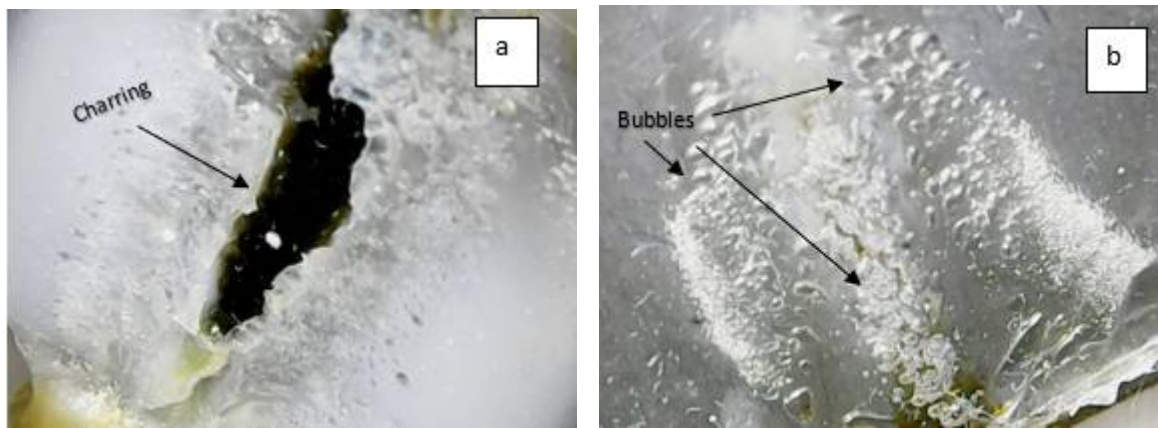
Figure 6: The digital macroscopic morphology of the strongest and weakest joint

Even though the sixth joint had the strongest joint, the PET charring in the middle of the joint shown in Figure (6a) resulted from the increased energy density.

During the tensile shear test, the PET part of the weakest joint was fractured from the middle of the joint along the welding line. On the contrary, the PET wasn't faced the same in the case of the strongest joint, where the fracture occurred directly after the joint took place. Both cases can be seen clearly in Figure (7).
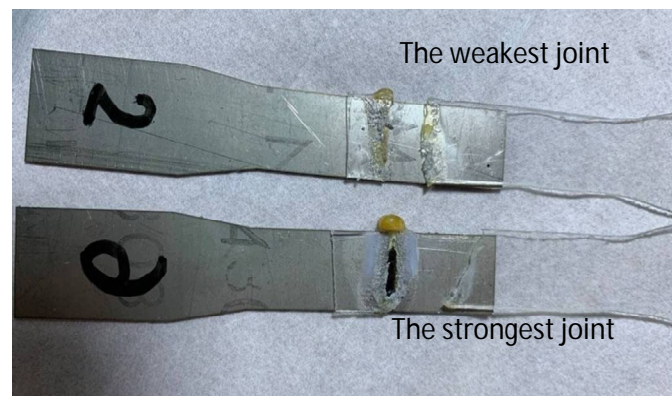
Figure 7: The strongest and weakest joints after the tensile shear test

The microscope's high-resolution pictures of the joints were taken, as shown in Figure (8). The best joint had a good-looking joint with a uniform and smooth interface between the SUS316 and PET. However, the worst joint witnessed a distortion in the polymer side.
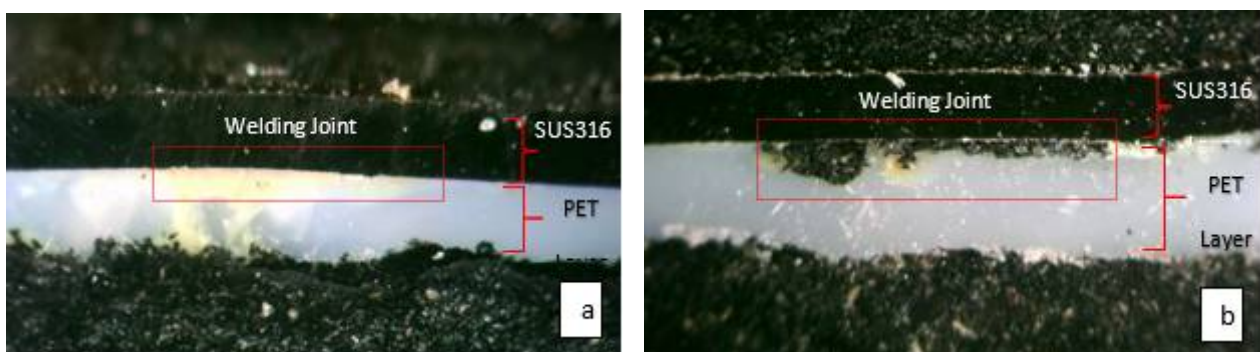
Figure 8: The microscope pictures the strongest and weakest joints

This study applied the laser conduction welding technique to achieve a dissimilar joining process between SUS316 and PET. A pulse Nd:YAG laser was used. The two materials were successfully joined in a lap joint using different welding parameters. These parameters were arranged and optimized by the Taguchi method. The effect of the welding parameters on the joint force was studied and discussed. Finally, a comparison between the strongest and the weakest joint was carried out. The following conclusions were reached in this study:

1) All the parameters affected the joint force. However, the energy density had the highest impact among the other parameters, followed by the pulse duration and the welding speed.

2) Taguchi method assisted in designing the experiment and finding the optimum set of parameters which were 250 J/cm^2 energy densities, 15 ms pulse duration, and 20 mm/min welding speed. The optimum parameters gave the maximum tensile force, which was 525 N.

3) A vast difference between the strongest and the weakest joint was quite apparent in the bubble formation, which weakened the force in the interface between the SUS316 and PET, which was evident in the weakest joint. This formation is attributed to the constriction of the melted polymer side in the joint.

Future work

Although the research found evidence of using Nd:YAG laser in joining SUS316 to PET within its scope, it is necessary to conduct further studies using other lasers such as diode laser or fiber laser and study the effects of these lasers' characteristics on the joining process. In addition, it is possible to do similar research using longer pulse durations starting from 20 ms and higher to study the effect of changing the pulse duration on joint force.

Author Contribution

All authors contributed equally to this work.

Funding

Data Availability Statement

The data that support the findings of this study are available on request from the corresponding author.

Conflicts of Interest

The authors declare that there is no conflict of interest.

References

[1] F. Lambiase, Mechanical behavior of polymer–metal hybrid joints produced by clinching using different tools, Mater. Des., 87 (2015) 606-618. https://doi.org/10.1016/j.matdes.2015.08.037

[2] J. Liu, W. Cui, Y. Shi, Hongyin Zhu, Zhong Li. Effect of surface texture and ultrasonic on tensile property of 316L/PET dissimilar joints, J. Manuf. Process., 50 (2020) 430-439. https://doi.org/10.1016/j.jmapro.2019.12.030

[3] R. Holtkamp, A. Roesner, A. Gillner. Advances in hybrid laser joining, J. Adv. Manuf. Technol., 47 (2010) 923-930. https://doi.org/10.1007/s00170-009-2124-6

[4] F. Yusof, M. Yukio, M. Yoshiharu, M. H. A. Shukor. Effect of anodizing on pulsed Nd: YAG laser joining of polyethylene terephthalate (PET) and aluminium alloy (A5052), Mater. Des., 37 (2012) 410-415. https://doi.org/10.1016/j.matdes.2012.01.006

[5] K. A.Hubeatir, Laser transmission welding of PMMA using IR semiconductor laser complemented by the Taguchi method and grey relational analysis, Mater. Today: Proc., 20 (2020) 466-473. https://doi.org/10.1016/j.matpr.2019.09.167

[6] Zhou J., Tsai, H. L. Developments in pulsed and continuous wave laser welding technologies, Handbook of Laser Welding Technologies, 2013. https://doi.org/10.1533/9780857098771.1.103

[7] E. Assuncao, S. Williams, D. Yapp. Interaction time and beam diameter effects on the conduction mode limit. Opt. Lasers Eng., 50 (2012) 823-828. https://doi.org/10.1016/j.optlaseng.2012.02.001

[8] H. Al-Kazzaz, M. Medraj, X. Cao, M. Jahazi. Nd: YAG laser welding of aerospace grade ZE41A magnesium alloy: Modeling and experimental investigations, Mater. Chem. Phys., 109 (2008) 61-76. https://doi.org/10.1016/j.matchemphys.2007.10.039

[9] A. M. Chelladurai, K. A. Gopal, S. Murugan, S. Venugopal, T. Jayakumar. Energy transfer modes in pulsed laser seam welding. Mater,Manuf. Process., 30 (2015) 162-168. https://doi.org/10.1080/10426914.2014.965829

[10] W. A. Ayoola, W. J. Suder, Stewart W. Williams. Parameters controlling weld bead profile in conduction laser welding, J. Mater. Process. Technol., 249 (2017) 522-530. https://doi.org/10.1016/j.jmatprotec.2017.06.026

[11] Klein, R. Laser welding of plastics: materials, processes and industrial applications,John Wiley & Sons, 2012. http://dx.doi.org/10.1002/9783527636969

[12] Kannatey-Asibu, Elijah, J.r. Principles of laser materials processing, John Wiley & Sons, 2009. http://dx.doi.org/10.1002%2F9780470459300

[13] E. M. Anawa, A. G. Olabi. Using Taguchi method to optimize welding pool of dissimilar laser-welded components. Opt. Laser Technol., 40 (2008) 379-388. https://doi.org/10.1016/j.optlastec.2007.07.001

[14] Y. Miyashita, M. Takahashi, M. Takemi, K. Oyama, Y. Mutoh, H. Tanaka. Dissimilar materials micro welding between stainless steel and plastics by using pulse YAG laser, J. Solid Mech., 3 (2009) 409-415. https://doi.org/10.1299/jmmp.3.409

[15] I. Hussein, Furat, E. Akman, B. Genc Oztoprak, M. Gunes, O. Gundogdu, E. Kacar, K. I. Hajim, A. Demir. Evaluation of PMMA joining to stainless steel 304 using pulsed Nd: YAG laser, Opt. Laser Technol., 49 (2013) 143-152. https://doi.org/10.1016/j.optlastec.2012.12.028

[16] Y. Huang, X.Gao, Y. Song, N.Zhang, N. Ma. Visual inspection of pulsed Nd: YAG laser welding of PMMA and stainless steel 304, 2017 IEEE International Conference on Imaging Systems and Techniques (IST), Beijing, China, 2017, 1-6. https://doi.org/10.1109/IST.2017.8261528

[17] L. Jia, , H. Yang, Y. Wang, B. Zhang, H. Liu, J. Hao. Research on temperature-assisted laser transmission welding of copper foil and polyethylene terephthalate, J. Manuf. Process., 57 (2020) 677-690. https://doi.org/10.1016/j.jmapro.2020.07.026

[18] S. P. Dwivedi, S. Sharma, V. Singh. Optimization of laser transmission joining process parameters on joint width of PET and 316 L stainless steel joint using RSM, J. Opt., 45 (2016) 106-113. https://doi.org/10.1155/2014/197060

[19] F. I. Al-Najjar, Evaluation of Weld Bead Width and Strength of PMMA Joining to st. st. 304 using Pulsed Nd: YAG Laser, Opt. Laser Technol.,49 (2013) 143-152. https://doi.org/10.1016/j.optlastec.2012.12.028

[20] F. M. Shaker, K. A. Hubeatir, M. M. AL-Khafaji. Effect of CW green laser parameters on welding width and strength of PMMA polymer. In AIP Conference Proceedings, AIP Publishing LLC., 2213,2020, 020192. https://doi.org/10.1063/5.0000276

[21] J. Imran, Hadeel, Kadhim A. Hubeatir, Mohanned M. Al-Khafaji. CO2 Laser Micro-Engraving of PMMA Complemented By Taguchi and ANOVA Methods, J. Phys.: Conf. Ser.,1795,2021, 012062. https://doi.org/10.1088/1742-6596/1795/1/012062

[22] J. Jiao, Q.Wang, F.Wang, S. Zan, W. Zhang,Numerical and experimental investigation on joining CFRTP and stainless steel using fiber lasers, J. Mater. Process. Technol., 240 (2017) 362-369. https://doi.org/10.1016/j.jmatprotec.2016.10.013

[23] F. S. Noh, H. M. Zin, K. Alnasser, N. Yusoff, F. Yusof. Optimization of laser lap joining between stainless steel 304 and Acrylonitrile Butadiene Styrene (ABS), Procedia Eng., 184 (2017) 246-250. https://doi.org/10.1016/j.proeng.2017.04.092